Regulatory mechanism of the six-method massage antipyretic process on lipopolysaccharide-induced fever in juvenile rabbits: A targeted metabolomics approach

Di Liu [a,b], Ying-qi Zhang [a], Tian-yuan Yu [a,*], Si-long Han [c,**], Ya-jing Xu [a], Qian Guan [a], Hou-rong Wang [a]

[a] School of Acupuncture-Moxibustion and Tuina, Beijing University of Chinese Medicine, Beijing, 102401, China
[b] Department of Acupuncture-Moxibustion, Dongfang Hospital Affiliated to Beijing University of Chinese Medicine, Beijing, 100078, China
[c] Department of Orthopedics II, Changping District Hospital of Integrated Traditional Chinese and Western Medicine, Beijing,102208, China

ARTICLE INFO

ABSTRACT

Objective: To investigate the mechanism of the six-method massage antipyretic process (SMAP) and its influence on the body's metabolic state.
Methods: The random number table method was used to divide 24 New Zealand 2-month-old rabbits with qualified basal body temperature into a control group, model group and massage group ($n = 8$ per group). The model group and massage groups were injected with 0.5 μg/ml lipopolysaccharide (1 ml/kg) into the auricular vein, and the control group was injected with the same amount of normal saline at the same temperature. One hour after modelling, the massage group was given SMAP (opening *Tianmen*, pushing *Kangong*, rubbing *Taiyang*, rubbing *Erhougaogu*, clearing the *Tianheshui* and pushing the spine). The change of anal temperature 5 h after moulding was recorded to clarify the antipyretic effect.
Results: After modelling, the rectal temperature of the juvenile rabbits in the three groups increased. The rectal temperature of the model group was higher than that of the control group 5 h after modelling, and the rectal temperature of the massage group was lower than that of the model group ($P < 0.05$). The antipyretic mechanism is related to the regulation of the synthesis of phenylalanine, tyrosine and tryptophan, as well as the pentose phosphate pathway. Compared with the model group, the plasma interleukin (IL)-1, IL-6, interferon-gamma, toll-like receptor 4, nuclear factor κB, the mechanistic target of rapamycin complex 1, indoleamine 2,3-dioxygenase 1, aryl hydrocarbon receptor, liver aspartate transaminase (AST), alanine transaminase (ALT) and L-glutamate dehydrogenase (L-GLDH) expression in the massage group were significantly decreased ($P < 0.05$). Compared with the model group, the massage group had significantly reduced AST, ALT and L-GLDH expression in plasma ($P < 0.05$).
Conclusion: The mechanism of SMAP therapy is related to regulating the expression of peripheral inflammatory factors and metabolic pathways.

* Corresponding author. School of Acupuncture-Moxibustion and Tuina, Beijing University of Chinese Medicine No. 11 Beisanhuan East Road, Chaoyang District, Beijing, 102401, China.
** Corresponding author. Department of Orthopedics II, Changping District Integrated Traditional Chinese and Western Medicine Hospital of Beijing, No.219 Huangping Road, Changping District, Beijing,102208, China.
E-mail addresses: yutianyuan9@126.com (T.-y. Yu), han44silong@21cn.com (S.-l. Han).

1. Introduction

Fever is a physiological process where the body regulates its temperature through local inflammatory responses or the action of neurotransmitters in response to infections or other stimuli. Children may exhibit the rapid onset of fever, fast progression and recurring symptoms due to partially developed immune and respiratory systems and other body-regulating functions [1]. Infantile fever is often caused by cold, food accumulation or other pathogenic factors. Drug therapy is ineffective in treating fever when the underlying cause of the illness is unknown [2]. Drug therapy is prone to developing resistance, affecting long-term effectiveness and producing side effects. Paediatric massage is regarded as an acceptable non-pharmaceutical therapy for children with optimal effects and has been widely used for infantile fever in China [2]. Compared with medication, it reduces drug dependence and the incidence of side effects. Additionally, massage therapy can promote children's self-regulation abilities, enhance immunity, increase antibody levels and positively affect disease prevention and treatment [2,3].

Metabolomics uses high-throughput analysis techniques to quantitatively and qualitatively analyse metabolic products (small organic molecules, metabolites, drugs, etc.) in organisms to explore the regulatory mechanisms of metabolic processes and their relationships with diseases [4]. The application of metabolomics technology involves aspects such as biochemical reactions of metabolites, metabolic pathways and metabolic regulation mechanisms. It can be used for discovering biological markers, monitoring disease diagnosis and treatment, drug metabolism research, detection of environmental pollutants and other areas [5]. Research has shown that massage therapy can affect biochemical indicators in plasma; however, there is still limited relevant research and more experiments and clinical studies are required to prove its effectiveness [6]. In detecting plasma metabolomics, the mechanism of massage therapy in reducing fever can be intuitively reflected.

To investigate the mechanism of the six-method massage antipyretic process (SMAP) and its influence on the body's metabolic state, this study used rabbits with lipopolysaccharide (LPS)-induced fever as the research object. The SMAP approach was applied, and non-targeted metabolomics was used to explore how SMAP influences the body's metabolic pathways. Enzyme-linked immunosorbent assay (ELISA) technology was adopted to detect the expression of inflammatory molecules and reveal their mechanism of fever reduction. This study enhances the understanding of the mechanism and efficacy of massage therapy and provides a scientific basis for its clinical application.

2. Materials and methods

Ethical approval

The study protocol was approved by the Animal Ethics Committee of the Beijing University of Chinese Medicine (BUCM-4-2020083102-3013).

2.1. Reagents and instruments

The reagents included lipopolysaccharide (Sigma), saline, sodium pentobarbital, methanol (Millipore), acetonitrile (C Millipore), ammonium acetate (Sigma), ammonia (Merck) and ultrapure water. Interleukin-1 (IL-1), IL-6, toll-like receptor 4 (TLR4), nuclear factor κB (NF-kB), mechanistic target of rapamycin complex 1 (mTORC1), indoleamine 2,3-dioxygenase 1 (IDO1), aryl hydrocarbon receptor (AhR), liver aspartate transaminase (AST), alanine transaminase (ALT), and L-glutamate dehydrogenase (L-GLDH). In terms of instruments, this included ELISA kits, an informational biosignal acquisition and processing system (BL-420 N, Chengdu Taimeng Technology Co., Ltd.), a temperature probe (CW100, Chengdu Taimeng Technology Co., Ltd.), an electronic balance (TCA 6 kg/1 g, Shuangjie [Brother] Group Co., Ltd., USA), an ultra-high pressure liquid chromatograph system (Shimadzu), a mass spectrometer (Thermo Scientific), a chromatographic column (Waters), a centrifuge (Eppendorf Centrifuge), balance (Sartorius), ultrasonic system (Diagenode) and vacuum centrifuge concentrator (Eppendorf).

2.2. Animal treatment

Clean grade 2-month-old New Zealand male rabbits, weighing 1.5–2.0 kg, with a rectal temperature of 39 °C ± 0.5 °C, were housed individually in separate cages at the animal centre for 3 days of acclimation. The baseline body temperature was measured at a fixed time every morning, while the rectal temperature was first measured after emptying the colon, followed by baseline temperature measurement while the rabbit was in a quiet state 5–10 min later. Three measurements were taken, and the average was obtained. Rabbits with temperatures of 38.5°C-39.5 °C, with a difference of no more than 0.4 °C between the highest and lowest temperatures, and no anal bleeding were identified as qualified young rabbits. The laboratory temperature was maintained at 25 °C ± 2 °C, with a humidity of 40%–60 %. The young rabbits were adapted to neck fixation, temperature measurement, imitation injection and blood sampling after removing them from the cage every morning at 8 a.m.

The 24 young rabbits were fasted without water for 12 h and were randomly divided into a control group, a model group and a massage group using a random number table, with eight rabbits in each group. The control group was injected with 1 mL/kg of saline via the auricular vein. The model and massage groups were injected with 0.5 µg/mL of LPS, 1 mL/kg via the auricular vein [7]. An information collection system was used to monitor and record the rectal temperature every 20 min. The model was successfully established if the rectal temperature increased by more than 0.5 °C within 1 h.

2.3. Massage method

The use of rabbits as the experimental animals was due to their larger volume compared with rats, allowing the operators to accurately select acupoints for massage. Massage on animals is currently a commonly used method for studying the mechanism of massage action [8]. The operation area for massage techniques in the control, model and massage group animals was shaved one day prior to the experiment. The massage was commenced at 8 a.m. After successful modelling, the massage group used room temperature water as a medium and followed the steps outlined below for the technique operation. ① First method: *Kai Tian Men* (straight push 200 times from the midpoint of the two eyebrows of the rabbit to the Shen Ting acupoint) for 2 min; ② second method: *Tui Kan Gong* (straight push 200 times from the inner corner of the rabbit's eye to the outer end of the upper eyelid junction) for 2 min; ③ third method: *Rou Tai Yang* (rub 200 times on the temple above the outer corner of the rabbit's eye) for 2 min [9]; ④ fourth method: *Rou Er Hou Gao Gu* (rub 24 times and pinch three times at the notch above the anterior edge of the rabbit's atlas wing) for 2 min; ⑤ fifth method: *Qing Tian He Shui* (500 times from the wrist crease to the elbow crease of the rabbit) for 5 min; and ⑥ sixth method: *Tui Ji* (The region from the midpoint of the rabbit's back to the coccyx between the seventh cervical vertebra and the first thoracic vertebra was straight pushed 300 times) for 5 min. During the same period, the model group and control group rabbits were rubbed with an equal amount of room temperature water on the shaved area to form the SMAP group but were not subjected to massage interventions. In control and model group, gentle force was applied only to the skin, not the subcutaneous tissue, ensuring the skin did not redden. The doctor kept their index and middle fingers together and maintained a clenched fist, applying even and consistent pressure. The shoulder, elbow and wrist joints remained relaxed, with flexion and extension movements executed by the elbow joint. The skin's surface should not be left during rubbing, and the forearm should drive the wrist in a rhythmic circular motion [9]. The frequency and duration of rubbing for the model and control groups matched those of the massage group.

All intervention measures were performed at the same time in the morning. The operator was certified as a licensed doctor and received uniform training to ensure the same operation and stimulation levels.

2.4. Efficacy evaluation

The body temperature was recorded every 20 min after modelling for 5 h. To do this, the perianal area of the rabbits was gently touched with a medical cotton swab. Once the rabbits had passed several stools, Vaseline was applied to an anal thermometer for lubrication. The thermometer probe, marked in advance to ensure a consistent insertion length, was then slowly inserted into the rectum to a depth of around 5 cm and was secured to the tail using adhesive tape.

2.5. Sampling

Approximately 5 h after modelling, 1 % sodium pentobarbital (30 mg/kg) was injected intraperitoneally, and blood was collected from the inferior vena cava by opening the abdomen after complete anaesthesia. Blood samples were left for 20 min at room temperature and then centrifuged at 2000 rpm for 10 min at 4 °C. The supernatant was taken to obtain plasma samples stored at −80 °C in the refrigerator for measurement. After the blood was taken from the abdominal aorta, the head was quickly severed, and the liver tissue was removed. The right lower lobe of the liver was cut uniformly according to the sampling standard (around 1 × 1 cm in size) cleaned up with saline and placed in liquid nitrogen.

2.6. Metabolite extraction

The samples were thawed at 4 °C and vortexed uniformly, and 100 μL of the sample was taken and mixed with 100 μL of pre-chilled water and 800 μL of pre-chilled methanol/acetonitrile (1:1, v/v). The mixture was homogenised and sonicated for 1 h in an ice bath, followed by incubation at −20 °C for 1 h to precipitate protein. The solution was then centrifuged at 16,000 g at 4 °C for 20 min, and the resulting supernatant was collected. The supernatant was dried using a high-speed vacuum concentrator prior to mass spectrometry analysis. For the analysis, 100 μL of methanol-water solution (1:1, v/v) was added to resuspend the sample, followed by centrifugation at 20,000 g and 4 °C for 20 min, and the resulting supernatant was collected for injection.

2.7. Liquid chromatography with tandem mass spectrometry analysis

2.7.1. Chromatographic separation

The samples were analysed using a SHIMADZU-LC30 ultra-high-performance liquid chromatography (UHPLC) system equipped with an ACQUITY UPLC® HSS T3 (2.1 × 100 mm, 1.8 μm) (Waters, Milford, MA, USA) chromatographic column. A 5-μL injection volume was used, and the column temperature was set at 40 °C with a flow rate of 0.3 mL/min. The chromatographic mobile phase consisted of solvent A, a 0.1 % formic acid aqueous solution, and solvent B, acetonitrile. The chromatographic gradient elution programme was as follows: 0–1.5 min with 0.3 % B; 1.5–2 min with a linear increase of B from 0.3 % to 0 %; 2–6 min with a linear increase of B from 0 % to 48 %; 6–10 min with a linear decrease of B from 48 % to 10 %; 10–12 min holding at 100 % B; 12–12.1 min with a linear decrease of B from 100 % to 0 %; and 12.1–15 min holding at 0 % B.

2.7.2. Mass spectrometry acquisition

Each sample was subjected to positive ion (+) and negative ion (−) mode detection using electrospray ionisation. After separation

via UHPLC, the samples were analysed using a QE Plus mass spectrometer (Thermo Scientific) with a heated electrospray ionisation source for ionisation. The ionisation conditions were as follows: spray voltage: 3.8 kv (+) and 3.2 kv (−); capillary temperature: 320 °C (±); sheath gas: 30 (±); aux gas: 5 (±); probe heater temperature: 350 °C (±); S-lens radio frequency level: 50(a.u.). The mass spectrometry acquisition was set as follows: mass spectrometry acquisition time: 15 min; range of parent ion scan: 70–1050 m/z; first-level mass resolution: 70,000 @m/z 200; automatic gain control (AGC) target: 3e6; first-level maximum IT: 100 ms. The second-level mass analysis was performed by triggering the acquisition of secondary mass spectrometry (MS^2) of the 10 highest-intensity parent ions after each full scan. Second-level mass resolution: 17,500 @m/z 200; AGC target: 1e5; second-level maximum IT: 50 ms; MS^2 activation type: higher-energy collision dissociation; isolation window: 2 m/z; normalised collision energy (Stepped): 10, 20, 30 eV.

2.7.3. Protein content detection in plasma via enzyme-linked immunosorbent assay

In accordance with the ELISA kit instructions, different concentrations of standard samples (50 μL) were added to the standard wells, and 40 μL of the sample dilution solution and 10 μL of the sample were added to the test sample wells. Then, 100 μL of enzyme-labelled reagent was added to each well, and the plate was sealed and incubated at 37 °C for 60 min. After washing each well five times, 50 μL of colour reagent A and 50 μL of colour reagent B were added, and the plate was kept in the dark for 15 min for colour development. Following this, 50 μL of stop solution was added to each well to terminate the reaction, and the optical density value was measured at a wavelength of 450 nm.

2.7.4. Statistical analysis

Peak alignment, retention time correction and peak area extraction of mass spectrometry data were performed using MS-DIAL software. Metabolite structural identification was performed by accurate mass matching (mass tolerance <20 ppm) and secondary spectrum matching (mass tolerance <0.02 Da), as well as through searching the Human Metabolome Database (HMDB), MassBank and other public databases and locally built metabolite standard libraries. For the extracted data, ion peaks with missing values within a group >50 % were not included in the subsequent statistical analysis. The total peak area was normalised for positive and negative ions separately, and the positive and negative ion peaks were integrated, with pattern recognition then performed using R software. The data were pre-processed by unit variance scaling for subsequent analysis.

A student's t-test and a one-way analysis of variance test were performed using SPSS software to compare and statistically analyse the differences in rectal temperature between groups. A P-value of <0.05 was considered to be statistically significant.

3. Results

3.1. Efficacy analysis

There was no significant change in rectal temperature in the control group of young rabbits. The comparison of rectal temperature between the massage group and the model group of young rabbits before modelling (0 h) and 1 h after modelling indicated no statistical significance ($P > 0.05$). However, at 2 and 3 h after modelling, the rectal temperature of the massage group was significantly lower than that of the model group ($P < 0.05$), indicating that massage therapy can effectively reduce the rectal temperature of LPS-induced fever in young rabbits (Table 1 and Fig. 1).

3.2. Orthogonal partial least squares discriminant analysis

The quality control samples were distributed centrally, and the data between control group and model group(Fig. 2a), the massage group and model group (Fig. 2b) were well distinguished. The samples of the massage and model groups were clearly separated, and the model had a good fit. The *R2Y* of the original model was very close to 1, indicating that the established model conformed to the actual situation of the sample data. The regression line of *Q2* was less than zero on the vertical axis. As the replacement retention rate gradually decreased, the proportion of the *Y* variable of the replacement increased, and the Q2 of the random model gradually decreased. This indicates that the original model has good robustness and no overfitting phenomenon.

3.3. Analysis of non-targeted differential metabolite expression

Fig. 3 shows the highly important differential metabolites between the control and model groups (Fig. 3a), as well as the model and massage groups(Fig. 3b) , with logarithmically transformed fold change on the *x*-axis and metabolites on the *y*-axis. The blue and

Table 1
Comparison of rectal temperature of young rabbits in different groups ($\bar{x} \pm s$).

Grouping	Results (°C)					
	0h	1h	2h	3h	4h	5h
Control group	39.01 ± 0.84	39.01 ± 0.11	38.91 ± 0.10	38.98 ± 0.12	39.01 ± 0.16	39.01 ± 0.11
Model group	38.99 ± 0.15*	40.04 ± 0.29*	40.40 ± 0.22*	40.90 ± 0.19*	40.75 ± 0.34*	40.14 ± 0.28*
Massage group	39.01 ± 0.11*#	40.01 ± 0.12*#	39.56 ± 0.47*#	39.94 ± 0.46*#	40.10 ± 0.39*#	39.74 ± 0.28*#

Note: Compared with the control group, *$P < 0.05$; Compared with the model group, #$P < 0.05$.
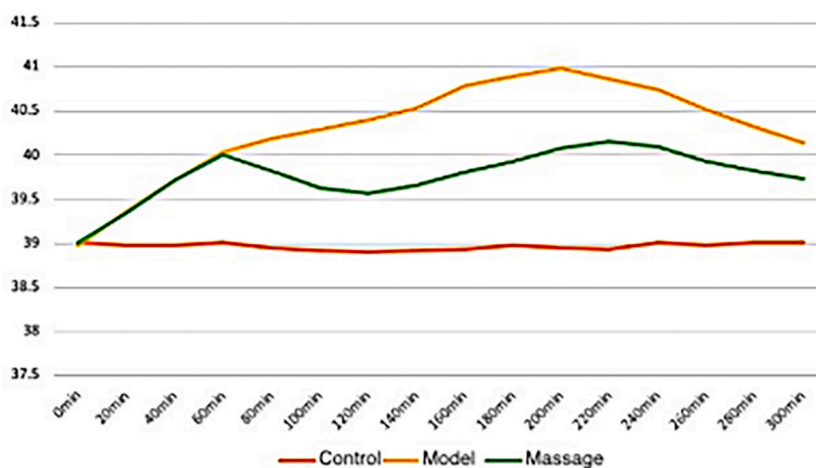
Fig. 1. Comparison of rectal temperature of young rabbits in different groups.

red dots on the left and right sides represent downregulated and upregulated differential metabolites, respectively. The size of the dots represents the variable importance in projection value, with larger dots indicating higher importance of the variable.

3.4. Analysis of Human Metabolome Database results for non-targeted differential metabolites

According to the HMDB statistical results shown in Fig. 4a, lipids and lipid-like molecules accounted for the highest proportion (30.77 %) among the differential metabolites between the model and control groups, followed by organic acids and their derivatives (21.15 %) and aromatic hydrocarbons (13.46 %).

According to the HMDB statistical results shown in Fig. 4b, lipids and lipid-like molecules accounted for the highest proportion (35.71 %) among the differential metabolites across the massage and model groups, followed by organic acids and their derivatives and organic oxygen compounds (21.43 %, 14.29 %).

3.5. Analysis of Kyoto Encyclopedia of Genes and Genomes results for non-targeted differential metabolites

According to the Kyoto Encyclopedia of Genes and Genomes (KEGG) annotation results, the level 1 pathways(Fig. 5a) that the differential metabolites across the model group and the control group belong to mainly include: 1. cellular processes; 2. environmental information processing; 3. genetic information processing; 4. human diseases; 5. metabolism; and 6. organismal systems. The level 2 KEGG pathways(Fig. 5b) are mainly enriched in the following: amino acid metabolism, cardiovascular diseases, cell growth and death, the digestive and endocrine systems, global and overview maps, immune diseases, the immune system, parasitic infectious diseases, membrane transport, other amino acid metabolism, the nervous system, neurodegenerative diseases, signal transduction, signalling molecules and their interactions and substance dependence and translation. The important pathways related to metabolism are the biosynthesis of valine, leucine and isoleucine; taurine and hypotaurine metabolism; glycine, serine and threonine metabolism; glutathione metabolism; cysteine and methionine metabolism; and amino acid biosynthesis and arginine biosynthesis.

According to the KEGG annotation results, the level 1 pathways(Fig. 6a) that the differential metabolites across the massage group and the model group belong to mainly include: 1. human diseases; 2. metabolism; and 3. organismal systems. The level 2 KEGG pathways(Fig. 6b) are mainly enriched in amino acid metabolism, cancer: overview, cancer: specific types, carbohydrate metabolism, digestive system, drug resistance: antineoplastic and the endocrine system. The important pathways related to metabolism include the biosynthesis of phenylalanine, tyrosine and tryptophan and the pentose phosphate pathway.

3.6. Analysis of flow paths of non-targeted differential metabolites and Kyoto Encyclopedia of Genes and Genomes pathways

Based on the Sankey diagram, compared with the control group, the differential metabolites that were upregulated and related to metabolism in the model group flowed as follows(Fig. 7a): the first part flowed into arginine biosynthesis, belonging to amino acid metabolism; the second part flowed into glycine, serine and threonine metabolism, belonging to amino acid metabolism; the third part flowed into valine, leucine and isoleucine biosynthesis, belonging to amino acid metabolism; the fourth and fifth parts flowed into amino acid biosynthesis, belonging to the whole and overview map; the sixth part flowed into glutathione metabolism, belonging to other amino acid metabolism; and the seventh part flowed into taurine and hypotaurine metabolism, belonging to other amino acid metabolism. The differential metabolites that were downregulated and related to metabolism flowed as follows: the first part flowed into arginine biosynthesis, belonging to amino acid metabolism; the second and third parts flowed into glycine, serine and threonine metabolism, belonging to amino acid metabolism; the fourth part flowed into valine, leucine and isoleucine biosynthesis, belonging to amino acid metabolism; the fifth and sixth parts flowed into amino acid biosynthesis, belonging to the whole and overview map; the
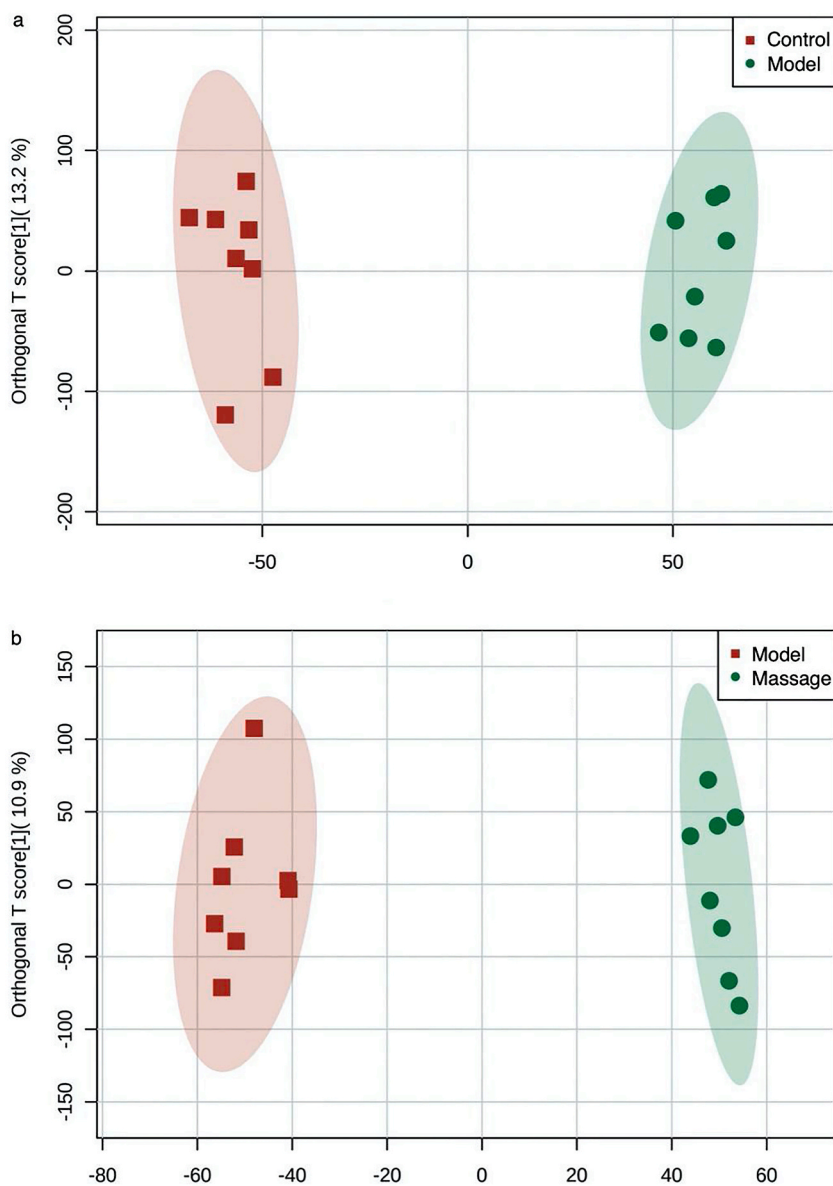
Fig. 2. (A) OrthogonalPartialLeast Squares-DiscriminantAnalysis(OPLS-DA) analysis of model group and control group; (b) OPLS-DA analysis of massage group and model group.

seventh part flowed into glutathione metabolism, belonging to other amino acid metabolism; and the eighth part flowed into taurine and hypotaurine metabolism, belonging to other amino acid metabolism.

Based on the Sankey diagram, compared with the model group, the differential metabolites that were upregulated and related to metabolism in the massage group flowed into the pentose phosphate pathway, belonging to carbohydrate metabolism(Fig. 7b). The differential metabolites that were downregulated and related to metabolism flowed into the biosynthesis of phenylalanine, tyrosine and tryptophan, belonging to amino acid metabolism.

3.7. Analysis of differential amino acid metabolism

The results showed that in the model group and the normal group, the histidine, valine, aspartic acid and tryptophan expressions were downregulated, with histidine exhibiting the most significant downregulation trend. In contrast, the expressions of tyrosine, serine, serine, proline, phenylalanine, methionine, lysine, leucine, isoleucine, L-glutamate, glycine, glutamine, cysteine, asparagine, arginine and alanine were upregulated, with tyrosine, serine and L-glutamate exhibiting the most significant upregulation trend(Fig. 8a
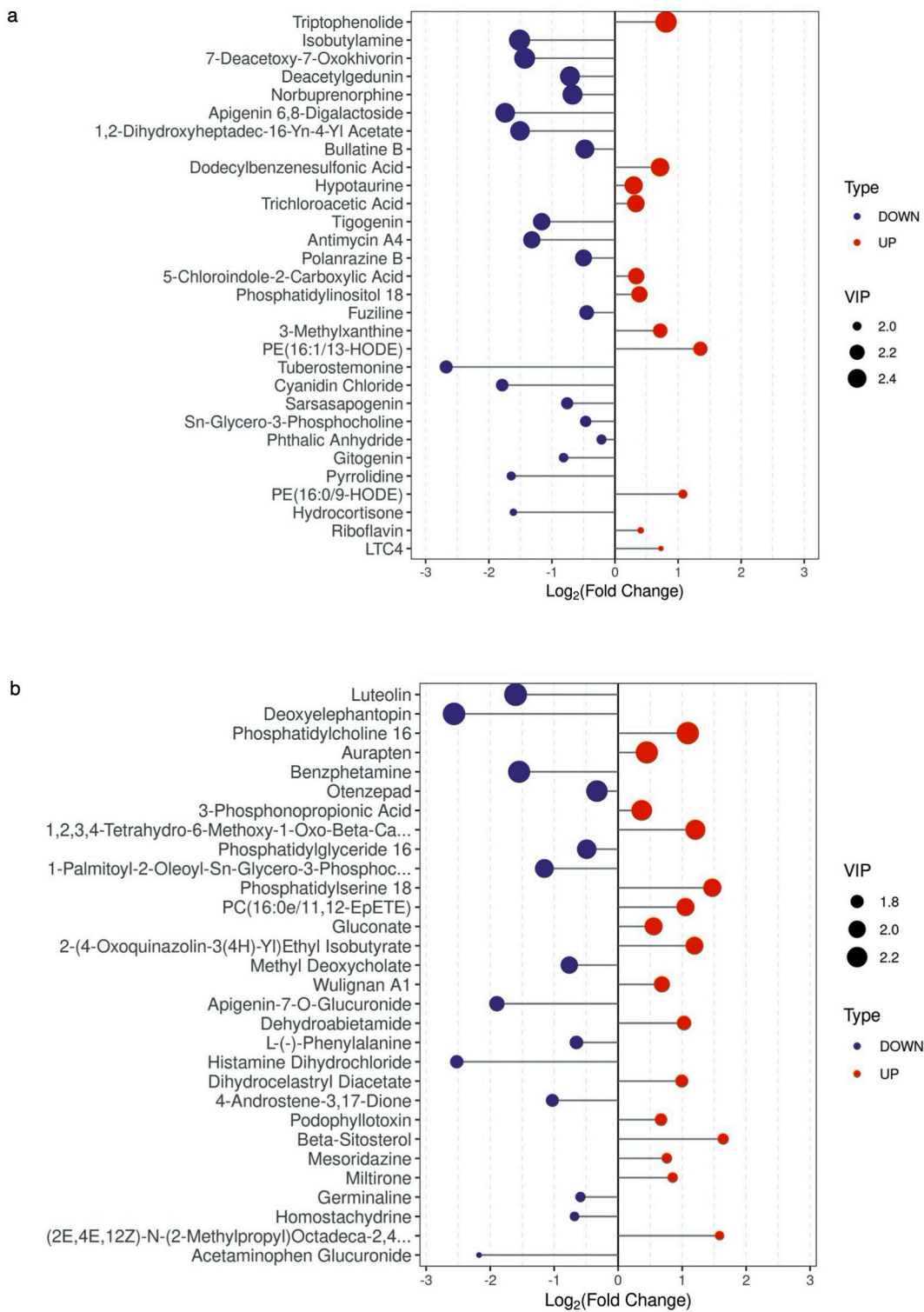
Fig. 3. (A) differential metabolite expression of model group and control group; (b) differential metabolite expression of massage group and model group.
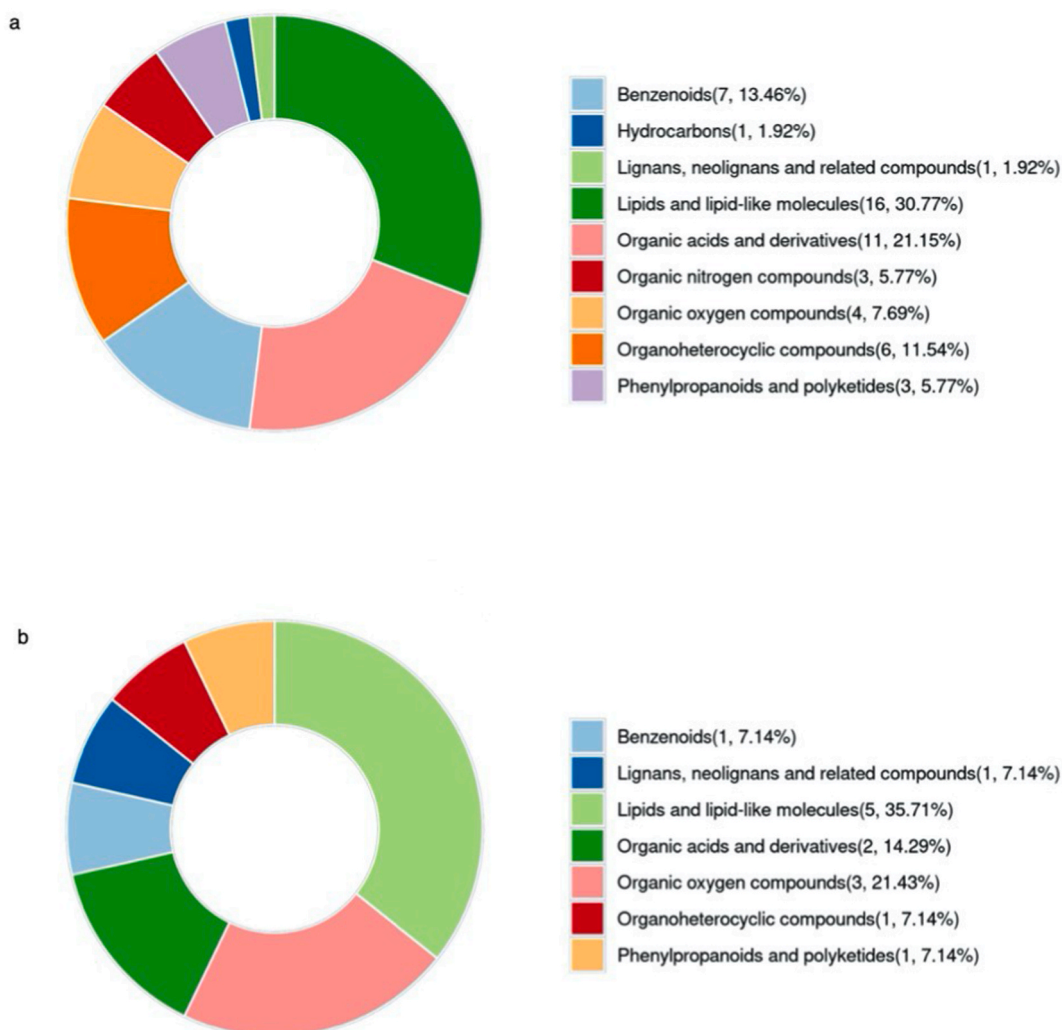
Fig. 4. (A) Hierarchical Circle Classification of differential metabolites of model group and control group (human Metabolome database: HM:DB); (b) Hierarchical Circle Classification of differential metabolites of massage group and model group (HMDB).

and b).

Furthermore, the results showed that in the massage and model groups, the expressions of tryptophan, serine and arginine were downregulated, with tryptophan exhibiting the most significant downregulation trend. Conversely, the expressions of histidine, valine, aspartic acid, tyrosine, serine, proline, phenylalanine, methionine, lysine, leucine, isoleucine, L-glutamate, glycine, glutamine, cysteine, asparagine, arginine and alanine were upregulated, with L-glutamate and cysteine exhibiting the most significant upregulation trend (Fig. 8c and d).

3.8. Changes in plasma indicators

The results showed that 5 h after modelling, the model group had higher expression of IL-1, IL-6, interferon-gamma (IFN-γ), TLR4, NF-kB, mTORC1, IDO1 and AhR in the plasma compared with the control group ($P < 0.05$). Compared with the model group, the massage group had significantly reduced expressions of IL-1, IL-6, IFN-γ, TLR4, NF-kB, mTORC1, IDO1 and AhR in the plasma ($P < 0.05$) (Tables 2–4).

3.9. Expression of aspartate transaminase, alanine transaminase and L-glutamate dehydrogenase in liver tissue

Here, the results indicated that 5 h after modelling, the model group had higher AST, ALT and L-DGLT expression in the plasma compared with the control group ($P < 0.05$). Compared with the model group, the massage group had significantly reduced AST, ALT and L-DGLT expression ($P < 0.05$) (Table 5).
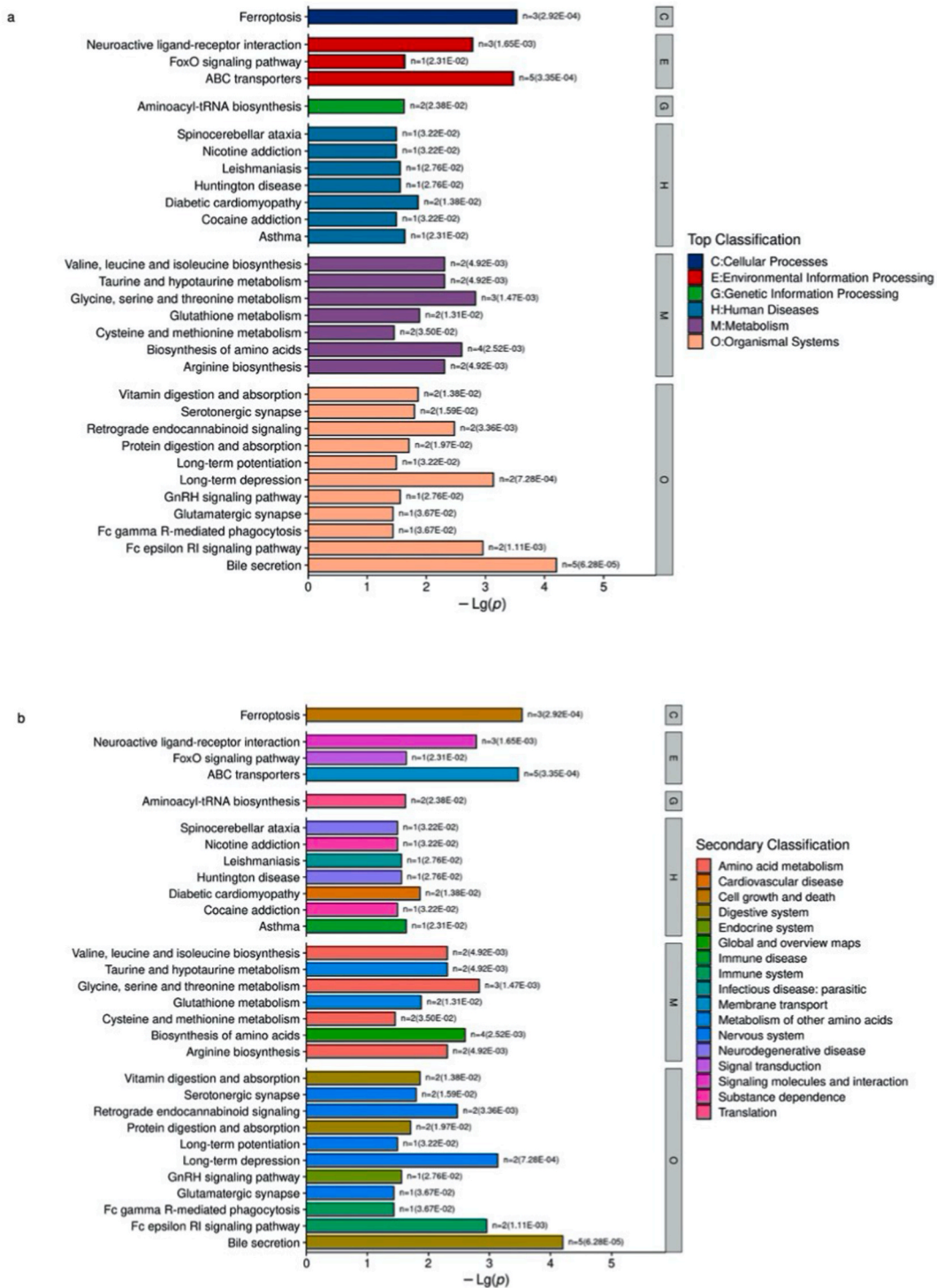
Fig. 5. (A) Histogram of Kyoto Encyclopedia of genes and Genomes(KEGG) pathway Enrichment of model group and control group (level 1); (b) Histogram of KEGG pathway Enrichment of model group and control group (level 2).
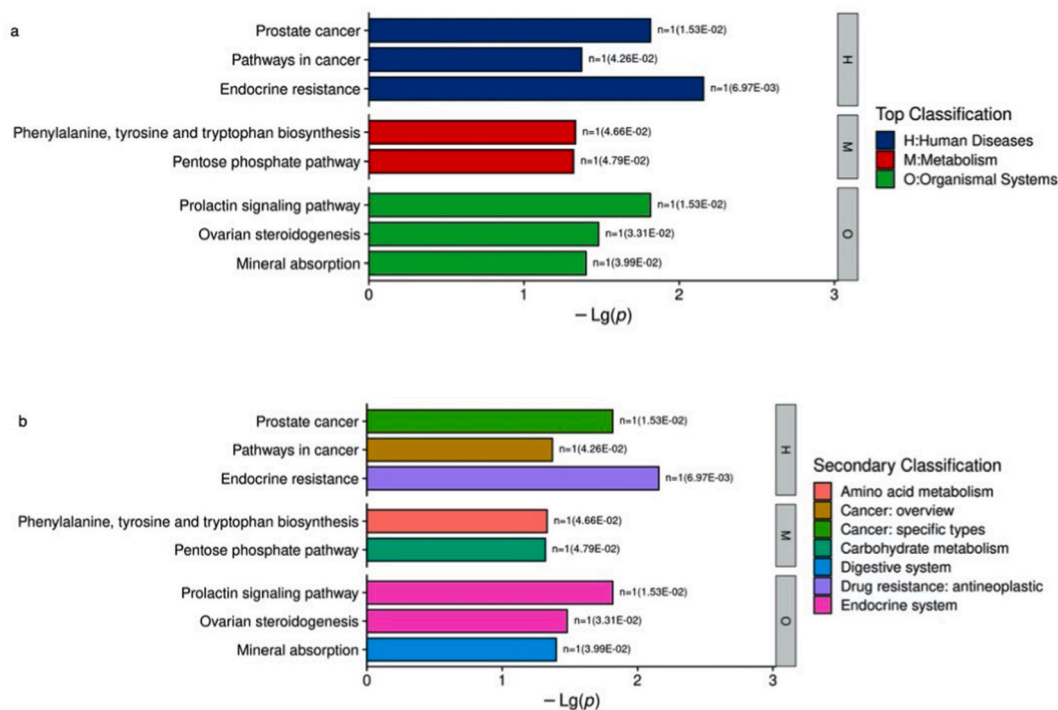
Fig. 6. (A) Histogram of KEGG pathway Enrichment of control group and model group (level 1); (b) Histogram of KEGG pathway Enrichment of massage group and model group (level 2) KEGG, Kyoto Encyclopedia of genes and Genomes.

4. Discussion

The research findings demonstrated that SMAP can effectively control the rectal temperature of rabbits with LPS-induced fever during both the rising and falling fever periods. Its antipyretic mechanism is related to the regulation of the synthesis of phenylalanine, tyrosine and tryptophan, as well as the pentose phosphate pathway. The antipyretic mechanism of massage therapy is related to the regulation of plasma IL-1, IL-6, IFN-γ, TLR4, NF-kB, mTORC1, IDO1 and AhR, as well as liver AST, ALT and L-GLDH expression.

Lipopolysaccharide is a molecule found in the outer membrane of gram-negative bacteria that can cause fever in the host. The immune system's reaction to LPS molecules usually mediates the process, including promoting inflammatory reactions through releasing cytokines and prostaglandin E2 (PGE2) [9]. While LPS-induced fever is a self-protective mechanism of the body, excessive or prolonged fever can negatively affect the body, including in terms of dehydration and metabolic stress. Therefore, fever needs to be finely regulated by the immune system [10].

Massage therapy can reduce muscle tension and stiffness, improving muscle flexibility [4]. It can also regulate the release of stress hormones such as cortisol, affecting amino acid metabolism [2]. Chronic stress can increase protein breakdown and decrease protein synthesis, resulting in a protein-negative balance. Massage therapy has been shown to reduce cortisol levels, improve protein balance and enhance amino acid metabolism [5]. In this study, there were significant changes in amino acid metabolism in the massage and model groups compared with the control group, indicating that both fever and massage can cause changes in amino acid metabolism.

In cellular metabolism, the phenylalanine and the pentose phosphate pathways can intersect and interact. For example, tyrosine produced in the phenylalanine pathway can enter further metabolism, such as the tricarboxylic acid cycle, through the pentose phosphate pathway to produce acetyl-CoA. Phenylalanine metabolism can interact with the pentose phosphate pathway, inducing mutual regulation under certain circumstances [11]. Therefore, in certain conditions, phenylalanine metabolism can affect the glyceraldehyde 3-phosphate dehydrogenase reaction in the pentose phosphate pathway and its adenosine triphosphate (ATP) production. Phenylalanine can also be transformed into tyrosine, catalysed by phenylalanine hydroxylase, which can further synthesise substances such as melanin [12]. This process requires nicotinamide adenine dinucleotide phosphate (NADPH) to provide reducing power within the cell, and NADPH is one of the important metabolic products of the pentose phosphate pathway.

Aromatic amino acids (AAAs), including phenylalanine, tyrosine and tryptophan, are essential amino acids that play important roles in protein synthesis and various metabolic pathways in the human body. They can regulate inflammation through multiple pathways. In addition, AAAs can be converted into neurotransmitters and hormones, directly or indirectly intervening in inflammation. They can serve as precursor molecules that are converted into a series of important lipid mediators, such as leukotrienes, thromboxane A2 and PGE2, which can lead to the occurrence and persistence of inflammation. Tryptophan is an essential amino acid required by the human body that cannot be synthesised internally and must be obtained through diet. More than 90 % of tryptophan is oxidised to produce urea through the kynurenine pathway, which involves multiple enzyme-catalysed reactions, resulting in various
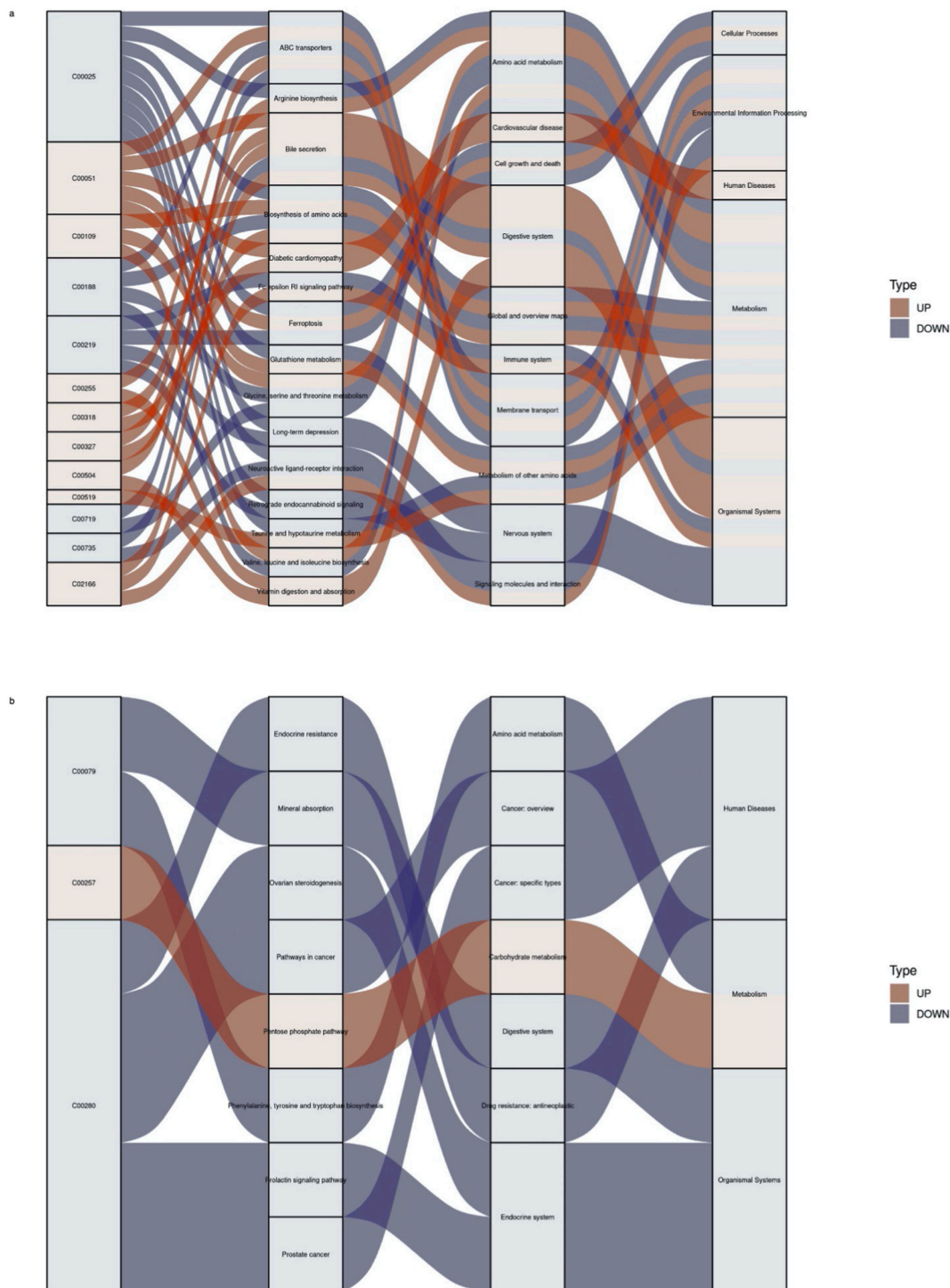
Fig. 7. (A) Sankey Diagram of Significant Pathway of Model Group and Control Group; (b) Sankey Diagram of Significant Pathway of Massage Group and Model Group (Note: The first column on the left represents the differential metabolites of up & down regulation, and the height of the box indicates the number of pathways annotated by the metabolites. The higher the box, the more pathways are annotated. The red flow line indicates the direction of up-regulated metabolites, and the blue flow line indicates the direction of down-regulated metabolites. The second, third, and fourth columns represent pathways in ascending order of hierarchy.). (For interpretation of the references to colour in this figure legend, the reader is referred to the Web version of this article.)
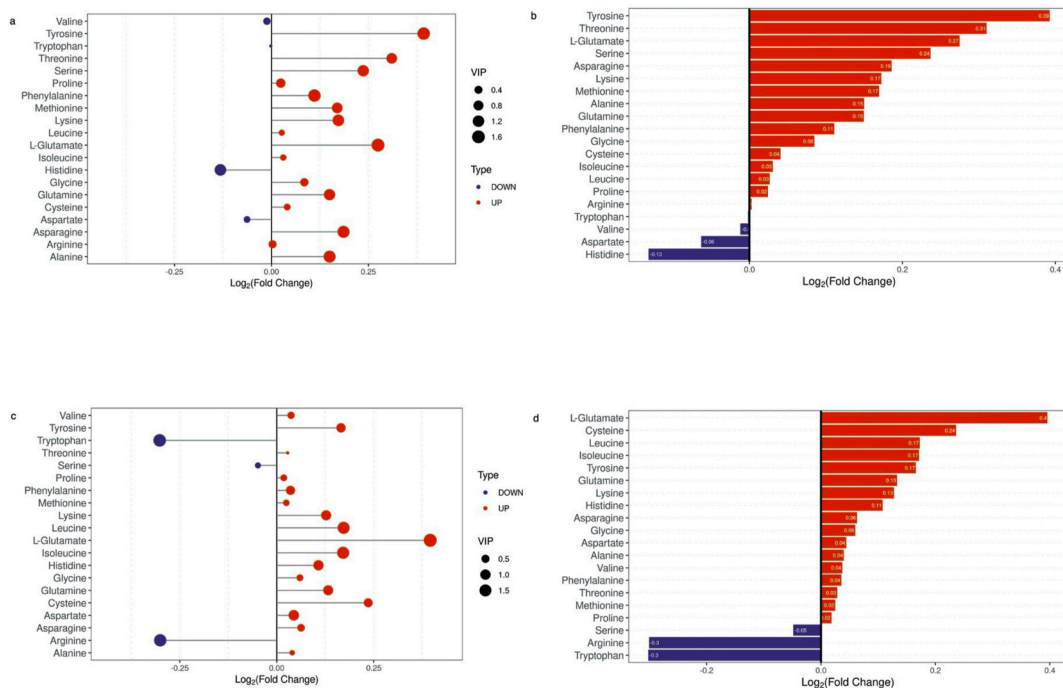
Fig. 8. (A) dot Plot of differential amino acids of model group and control group; (b) Histogram of differential amino acids of model group and control group; (c) dot Plot of differential amino acids of massage group and model group; (d) Histogram of differential amino acids of massage group and model group.

Table 2
Comparison of IL-1, IL-6, and IFN-γ Content in plasma of young rabbits in different groups ($\overline{x} \pm s$).

Grouping	IL-1β(ng/L)	IL-6(ng/L)	IFN-γ(ng/L)
Control group	102.976 ± 2.923	198.908 ± 8.737	921.859 ± 41.484
Model group	122.362 ± 4.918[a]	243.981 ± 8.280[a]	1064.940 ± 42.576[a]
Massage group	111.126 ± 9.229[ab]	216.537 ± 4.181 [ab]	962.376 ± 39.100 [ab]

Note: Compared with the control group, [a]$P < 0.05$; Compared with the model group, [b]$P < 0.05$.IL-1: interleukin-1; IL-6: interleukin-6; IFN-γ: Interferon-γ.

Table 3
Comparison of TLR4, NF-kB, and mTORC1 Content in Plasma of Young Rabbits in Different Groups ($\overline{x} \pm s$).

Grouping	TLR4(ug/L)	NF-κB(ng/L)	mTORC1(ng/L)
Control group	19.498 ± 0.654	2188.704 ± 110.634	170.359 ± 5.566
Model group	22.697 ± 0.862[a]	2471.965 ± 70.409[a]	193.386 ± 8.739[a]
Massage group	19.715 ± 0.737[ab]	2371.261 ± 106.516[ab]	180.947 ± 8.147[ab]

Note: Compared with the control group, [a]$P < 0.05$; Compared with the model group, [b]$P < 0.05$.TLR4:toll-like receptor 4; NF-κB: nuclear factor κB; mTORC1：the mechanistic target of rapamycin complex 1.

Table 4
Comparison of Ido1 and AhR Content in plasma of young rabbits in different groups ($\overline{x} \pm s$).

Grouping	IDO1(ng/L)	AhR(ng/L)
Control group	498.62 ± 15.304	1307.796 ± 52.849
Model group	592.055 ± 12.492[a]	1500.433 ± 59.336[a]
Massage group	503.942 ± 20.285[ab]	1352.005 ± 66.525[ab]

Note: Compared with the control group, [a]$P < 0.05$; Compared with the model group, [b]$P < 0.05$.IDO1: indoleamine 2,3-dioxygenase 1; AhR: aryl hydrocarbon receptor.

Table 5

Comparison of IL-1, IL-6, and IFN-γ Content in plasma of young rabbits in different groups ($\overline{x} \pm s$).

Grouping	AST(ng/L)	ALT(ng/L)	L-GLDH(ng/L)
Control group	154.122 ± 4.766	90.148 ± 3.604	206.195 ± 7.326
Model group	177.362 ± 7.219^a	108.199 ± 5.056^a	248.555 ± 10.194^a
Massage group	157.706 ± 8.027^{ab}	96.467 ± 4.314^{ab}	216.838 ± 9.224^{ab}

Note: Compared with the control group, $^aP < 0.05$; Compared with the model group, $^bP < 0.05$.AST: aspartate transaminase; ALT:alanine transaminase; L-GLDH:L-glutamate dehydrogenase.

metabolites that have important physiological and pathological effects [13]. Arginine metabolism plays an important role in the inflammatory response, as it can alleviate inflammation by reducing oxidative stress and NF-κB pathway activation induced by LPS in inflammation response [3]. Arginine can be hydrolysed to ornithine cysteine and alanine, which produce ornithine. These compounds are the main raw materials of certain inflammation mediators and antioxidants. Some amino acid transporters are receptors featuring both transport and sensing, triggering downstream signalling pathways, such as the mTORC1 pathway and the general control non-derepressible kinase pathway [14].

In this study, phenylalanine, tyrosine and tryptophan biosynthesis were downregulated in the massage group compared with the model group, and the pentose phosphate pathway and arginine metabolism were upregulated, indicating that massage therapy can suppress inflammatory reactions.

Aryl hydrocarbon receptor and IDO are two molecules that interact with each other and participate in regulating immune responses. When AhR is activated by its ligands, it can induce IDO expression in various cell types, such as dendritic cells, macrophages and endothelial cells [15]. Meanwhile, IDO can catalyse the conversion of tryptophan into an immunoregulatory metabolite, kynurenine, while AhR activation and subsequent induction of IDO expression can suppress immune responses by depleting tryptophan needed for T cell proliferation and function. This mechanism is believed to play a role in promoting immune tolerance and preventing autoimmunity.

The tryptophan catabolism of IDO1 in dendric cells (DCs) is a highly universal adaptive immune response regulator. By degrading tryptophan, IDO1 can suppress T cell proliferation and activation, playing a crucial role in regulating immune responses and maintaining immune homeostasis [16]. In an inflammatory environment characterised by strong immune activation, IFN-γ acts in a feedback manner to induce the enzymatic function of IDO1 through the combined effects of tryptophan starvation and tryptophan catabolites, thus preventing potential excessive reactions. The increased levels of IDO1 in LPS-stimulated DCs lead to an increase in kynurenine secretion. This known tryptophan degradation product inhibits the differentiation of pro-inflammatory T cells mediated by DCs and stimulates the proliferation of regulatory T cells. Induction of IDO1 requires interferons and cytokines, especially IFN-γ [17]. The TLR4 signalling pathway induced by LPS in DCs results in higher levels of IDO subtypes and AhR transcription factors [18].

Interleukin-1 beta was the first discovered inflammatory factor [16]. It is mainly produced by macrophages and its secreted form is closely related to fever. It can act on the central nervous system to cause fever through blood and body fluid pathways in synergy with IL-6, TNF-alpha (α) and IFN.

Interleukin-6 is a key cytokine in the inflammatory response, driving a core temperature rise as the primary mediator and acting as a downstream cytokine to coordinate lymphocyte transport. It is produced by various cells in response to infection, injury or tissue damage and serves as a critical mediator of inflammation. Interleukin-6 binds to its receptor and is expressed on many different cell types, activating various downstream signalling pathways, ultimately leading to inflammation. One of the main mechanisms of IL-6 in the inflammatory response is its ability to recruit and activate immune cells. It promotes the migration of immune cells, such as neutrophils and macrophages, to the site of inflammation. Once at the site, these cells are activated by IL-6, resulting in the production of other cytokines and chemokines and amplifying the inflammatory response [11].

The experimental results indicated that 5 h after the modelling, the expression of IL-6 in the massage group decreased and was significantly different from that in the model group, indicating that massage therapy can effectively reduce the expression of inflammatory factor IL-6 while decreasing body temperature. Combined with the non-targeted metabolomics detection results, the massage group upregulated differential metabolites entering the pentose phosphate pathway, suggesting that massage may intervene in glucose aerobic oxidation to produce acetyl-CoA expression by regulating the pentose phosphate pathway, reducing histone acetylation at the IL-6 promoter and downregulating IL-6 expression.

Interferon-γ is crucial in the immune system's response to inflammation and infection. It is produced by activated T cells and natural killer cells and acts by binding to specific receptors on the surface of target cells. Interferon-γ stimulates macrophages to increase their phagocytic activity, aiding in the clearance of pathogens from infected tissues. It also enhances the production of reactive oxygen and nitrogen species, assisting in eliminating intracellular pathogens [19]. Interferon-γ is a lymphokine with strong immune regulatory properties that can stimulate the production of other pro-inflammatory cytokines, such as IL-1 and TNF-α, aiding in the recruitment and activation of immune cells and promoting the inflammatory response. It can induce the synthesis of IDO1, which is involved in tryptophan catabolism. Interferon-γ can also induce M1 polarisation of macrophages through the glycolytic pathway, and 2-Deoxy-D-glucose glycolysis can inhibit IFN-γ-induced JAK-STAT1 activation by reducing ATP production [12].

Toll-like receptors are a family of innate immune system cell-expressed receptors stimulated by specific structural motifs expressed by bacteria, viruses and fungi, known as pathogen-associated molecular patterns [17]. When the TLR pathway is activated, NF-κB is subsequently activated and translocated to the cell nucleus, inducing various inflammatory cytokines, such as IL-1β, IL-6 and TNF-α. In addition to the TLR4-mediated role, NF-κB is a transcription factor that plays an important role in inflammation, immunity and cell

proliferation, differentiation and survival [2]. Activation of the NF-κB signalling pathway induces the release of inflammatory cytokines such as IL-1β, IL-6 and TNF-α [20]. The NLRP3 inflammasome recognises pathogens and related molecules through TLR to activate the NF-κB pathway, thereby promoting the transcription of NLRP3 and IL-1β. Nuclear factor-κB p65 is the downstream effector of TLR4. When TLR4 interacts with MyD88 in a ligand-dependent manner, it is translocated from the cytoplasm to the nucleus, where it binds to deoxyribonucleic acid to regulate the transcription of various cytokines, including IL-1β, IL-6 and TNF-α. Therefore, the TLR4/NLRP3/NF-κB p65 signalling pathway plays an important role in inflammatory signal transduction [12]. Lipopolysaccharide can activate the TLR4/MyD88/NF-κB pathway in RAW 264.7 macrophages and stimulate the upregulation of NLRP3 inflammasomes and IL-1β and IL-18 expression [19].

The mechanistic target of rapamycin complex 1 is a conserved serine/threonine protein kinase in evolution, belonging to the phosphoinositide 3-kinases-related kinase superfamily, which regulates cell growth and metabolism by regulating protein and lipid synthesis, lysosome biogenesis and autophagy. Signalling through mTORC1 can regulate the expression of genes involved in glycolysis, the pentose phosphate pathway, lipid biogenesis and pyrimidine biosynthesis [21]. Activated mTORC1 upregulates the synthesis of cellular building blocks (including proteins, lipids and nucleotides), shifting the metabolic programme of the cell from catabolism to anabolism [12].

The mechanistic target of rapamycin complex 1 can regulate inflammation by modulating immune cell metabolism. The activation of mTORC1 can stimulate glycolytic and mitochondrial metabolism in immune cells, resulting in increased ATP production and reactive oxygen species generation. By modulating various signalling pathways involved in nutrient sensing and metabolic homeostasis, mTORC1 can also regulate energy metabolism. Additionally, it can influence inflammatory responses by modulating the activity of transcription factors such as NF-κB and hypoxia-inducible factor-1α (HIF-1α) [22]. Activation of mTORC1 can promote the nuclear translocation and activity of NF-κB, a key regulatory factor of the inflammatory response, resulting in pro-inflammatory cytokine and chemokine production. Similarly, mTORC1 can stabilise and activate HIF-1α, promoting the expression of inflammatory and metabolic-related genes. Nuclear factor κ-B and NLRP3 inflammasomes are two key pathways involved in M1 polarisation [20]. In addition, mTORC1 and HIF-1α signalling are associated with macrophage polarisation.

The experimental results revealed that 5 h after moulding, the TLR4 and NF-kB expressions in the massage group were significantly downregulated compared with the model group, indicating that massage can reduce the expression of inflammatory factors by inhibiting the TLR4/NF-kB pathway, which is consistent with the previous results obtained by the research team. The mTORC1 expression was significantly downregulated in the massage group compared with the model group. Combined with the metabolomics results, the phosphogluconate pathway was identified as a differential metabolic pathway in the massage group, and arginine expression was downregulated. Therefore, it is suggested that massage therapy can regulate the metabolic process to inhibit the expression of mTORC1 and regulate the inflammatory response.

The most important transaminases involved in amino acid transamination are ALT and AST. The former mainly exists in the liver, while the latter exists in many tissues, including the liver, heart and muscle. In the transamination process, ALT catalyses the amino group to transfer from amino acids (such as alanine) to α-ketoglutarate, forming glutamic and pyruvic acid. Then, glutamic acid is further deaminated to form ammonium ions bound to urea for excretion [23]. Pyruvate can be used in various metabolic pathways, including gluconeogenesis, to produce glucose. Furthermore AST catalyses the transfer of amino groups from amino acids (such as aspartic acid) to α-ketoglutaric acid, forming glutamic acid and oxaloacetic acid. Glutamic acid is then further deaminated as described above, and oxaloacetic acid can be used in various metabolic pathways, including glucose production through gluconeogenesis. Transaminases play a crucial role in the joint deamination of amino acids by promoting the transfer of amino groups to α-ketones, leading to the production of energy, glucose and other metabolic intermediates [24].

5. Conclusion

The six-method massage antipyretic process can effectively control the pyrogenic effect of LPS during both the rise and fall of fever. Its antipyretic mechanism is related to regulating peripheral inflammation factors expression and metabolic pathways.

Advantages, deficiencies and prospects

This study explored the regulatory mechanism of massage on LPS-induced fever in young rabbits using targeted metabolomics, identifying several metabolic pathways. One strength of this study is its unique approach. We believe that changes in metabolic pathways are both causal and consequential in the development of diseases and are jointly regulated by multiple systems within the body. However, the study involves a number of limitations. First, the metabolic pathways identified are not typically associated with inflammation and fever, necessitating further research. Second, the correlation between this study's metabolomics results and other findings is not robust enough to provide evidence to strongly support other indices.

Ethics approval and consent to participate

The study protocol was approved by the Animal Ethics Committee of Beijing University of Chinese Medicine (BUCM-4-2020083102-3013).

Consent for publication

Not applicable.

Availability of data and materials

All data generated or analysed during this study are included in this article. **Competing interests**.
All of the authors had no any personal, financial, commercial, or academic conflicts of interest separately.

CRediT authorship contribution statement

Di Liu: Conceptualization, Formal analysis, Supervision, Writing – original draft, Writing – review & editing. **Ying-qi Zhang:** Data curation, Formal analysis, Investigation, Writing – review & editing. **Tian-yuan Yu:** Data curation, Formal analysis, Investigation, Writing – review & editing. **Si-long Han:** Data curation, Formal analysis, Investigation, Writing – review & editing. **Ya-jing Xu:** Data curation, Formal analysis, Investigation, Writing – review & editing. **Qian Guan:** Data curation, Formal analysis, Investigation, Writing – review & editing. **Hou-rong Wang:** Data curation, Formal analysis, Investigation, Writing – review & editing.

Declaration of competing interest

The authors declare that they have no known competing financial interests or personal relationships that could have appeared to influence the work reported in this paper.

References

[1] G.S. Marshall, Prolonged and recurrent fevers in children, J. Infect. 68 (Suppl 1) (2014 Jan) S83–S93, https://doi.org/10.1016/j.jinf.2013.09.017.
[2] L.F. Chen, M. Yin, X. Dong, J.X. Zou, B.X. Wang, J. Chen, Pediatric tuina for the treatment of fever in children: a protocol for systematic review and meta-analysis, Medicine (Baltim.) 99 (33) (2020 Aug 14), e21664, https://doi.org/10.1097/MD.0000000000021664.
[3] F. Wang, G.W. Cui, L. Kuai, J.M. Xu, T.T. Zhang, H.J. Cheng, H.S. Dong, G.R. Dong, Role of acupoint area collagen fibers in anti-inflammation of acupuncture lifting and thrusting manipulation, Evid Based Complement Alternat Med 2017 (2017), 2813437, https://doi.org/10.1155/2017/2813437.
[4] B.Y. Zhu, X. Li, P.D. Liao, [Academic features of tuina for children in western Hunan district], Zhongguo Zhen Jiu 32 (6) (2012 Jun) 548–550. Chinese. PMID: 22741266.
[5] Z.J. Cheng, S.P. Zhang, Y.J. Gu, Z.Y. Chen, F.F. Xie, C. Guan, M. Fang, F. Yao, Effectiveness of tuina therapy combined with yijinjing exercise in the treatment of Nonspecific chronic neck Pain: a randomized clinical trial, JAMA Netw. Open 5 (12) (2022 Dec 1), e2246538, https://doi.org/10.1001/jamanetworkopen.2022.46538.
[6] S.C. Chen, J. Yu, H.S. Wang, D.D. Wang, Y. Sun, H.L. Cheng, L.K. Suen, W.F. Yeung, Parent-administered pediatric Tuina for attention deficit/hyperactivity disorder symptoms in preschool children: a pilot randomized controlled trial embedded with a process evaluation, Phytomedicine 102 (2022 Jul 20), 154191, https://doi.org/10.1016/j.phymed.2022.154191.
[7] S.D. Zhang, S.H. Li, D.S. Wang, C.Z. Gong, H.S. Li, J.Y. Li, X. Li, Z.T. Yan, Fever effect of intravenous LPS on rabbits and SDS-PAGE comparative analysis of liver protein, Hubei Agric. Sci. 50 (7) (2011) 1416–1419, https://doi.org/10.3969/j.issn.0439-8114.2011.07.037.
[8] C. Wang, J.C. Zhu, Y.Z. Xiong, X.F. Ma, Z.W. Zheng, Y. Nie, Y.C. Li, Y. Su, [Experimental study on improvement of blood supply timeliness of rabbits with vertebral artery type of cervical spondylosis by massage], Zhong Guo Gu Shang 31 (8) (2018 Aug 25) 769–774, https://doi.org/10.3969/j.issn.1003-0034.2018.08.016. Chinese.
[9] N.S. Kim, T. Torres, W. Langridge, LPS enhances CTB-INSULIN induction of Ido1 and IL-10 synthesis in human dendritic cells, Cell. Immunol. 338 (2019 Apr) 32–42, https://doi.org/10.1016/j.cellimm.2019.03.003.
[10] J.L. Jewell, R.C. Russell, K.L. Guan, Amino acid signalling upstream of mTOR, Nat. Rev. Mol. Cell Biol. 14 (3) (2013 Mar) 133–139, https://doi.org/10.1038/nrm3522.
[11] P.K. Langston, A. Nambu, J. Jung, M. Shibata, H.I. Aksoylar, J. Lei, P. Xu, M.T. Doan, H. Jiang, M.R. MacArthur, X. Gao, Y. Kong, E.T. Chouchani, J.W. Locasale, N.W. Snyder, T. Horng, Glycerol phosphate shuttle enzyme GPD2 regulates macrophage inflammatory responses, Nat. Immunol. 20 (9) (2019 Sep) 1186–1195, https://doi.org/10.1038/s41590-019-0453-7.
[12] R. Chen, J. Wang, X. Dai, S. Wu, Q. Huang, L. Jiang, X. Kong, Augmented PFKFB3-mediated glycolysis by interferon-γ promotes inflammatory M1 polarization through the JAK2/STAT1 pathway in local vascular inflammation in Takayasu arteritis, Arthritis Res. Ther. 24 (1) (2022 Dec 12) 266, https://doi.org/10.1186/s13075-022-02960-1.
[13] F. Wang, S. Zhang, R. Jeon, I. Vuckovic, X. Jiang, A. Lerman, C.D. Folmes, P.D. Dzeja, J. Herrmann, Interferon gamma induces reversible metabolic reprogramming of M1 macrophages to sustain cell viability and pro-inflammatory activity, EBioMedicine 30 (2018 Apr) 303–316, https://doi.org/10.1016/j.ebiom.2018.02.009.
[14] M. Rebsamen, G. Superti-Furga, SLC38A9: a lysosomal amino acid transporter at the core of the amino acid-sensing machinery that controls MTORC1, Autophagy 12 (6) (2016 Jun 2) 1061–1062, https://doi.org/10.1080/15548627.2015.1091143.
[15] F. Bauernfeind, A. Ablasser, E. Bartok, S. Kim, J. Schmid-Burgk, T. Cavlar, V. Hornung, Inflammasomes: current understanding and open questions, Cell. Mol. Life Sci. 68 (5) (2011 Mar) 765–783, https://doi.org/10.1007/s00018-010-0567-4.
[16] D. De Nardo, C.M. De Nardo, E. Latz, New insights into mechanisms controlling the NLRP3 inflammasome and its role in lung disease, Am. J. Pathol. 184 (1) (2014 Jan) 42–54, https://doi.org/10.1016/j.ajpath.2013.09.007.

[17] S. Torretta, A. Scagliola, L. Ricci, F. Mainini, S. Di Marco, I. Cuccovillo, A. Kajaste-Rudnitski, D. Sumpton, K.M. Ryan, S. Cardaci, D-mannose suppresses macrophage IL-1β production, Nat. Commun. 11 (1) (2020 Dec 11) 6343, https://doi.org/10.1038/s41467-020-20164-6.

[18] M.A. Lauterbach, J.E. Hanke, M. Serefidou, M.S.J. Mangan, C.C. Kolbe, T. Hess, M. Rothe, R. Kaiser, F. Hoss, J. Gehlen, G. Engels, M. Kreutzenbeck, S. V. Schmidt, A. Christ, A. Imhof, K. Hiller, E. Latz, Toll-like receptor signaling rewires macrophage metabolism and promotes histone acetylation via ATP-citrate lyase, Immunity 51 (6) (2019 Dec 17) 997–1011.e7, https://doi.org/10.1016/j.immuni.2019.11.009.

[19] X. Meng, X. Zhang, X. Su, X. Liu, K. Ren, C. Ning, Q. Zhang, S. Zhang, Daphnes Cortex and its licorice-processed products suppress inflammation via the TLR4/ NF-κB/NLRP3 signaling pathway and regulation of the metabolic profile in the treatment of rheumatoid arthritis, J. Ethnopharmacol. 283 (2022 Jan 30), 114657, https://doi.org/10.1016/j.jep.2021.114657.

[20] P. Xiang, T. Chen, Y. Mou, H. Wu, P. Xie, G. Lu, X. Gong, Q. Hu, Y. Zhang, H. Ji, NZ suppresses TLR4/NF-κB signalings and NLRP3 inflammasome activation in LPS-induced RAW264.7 macrophages, Inflamm. Res. 64 (10) (2015 Oct) 799–808, https://doi.org/10.1007/s00011-015-0863-4.

[21] J. Muri, H. Thut, Q. Feng, M. Kopf, Thioredoxin-1 distinctly promotes NF-κB target DNA binding and NLRP3 inflammasome activation independently of Txnip, Elife 9 (2020 Feb 25), e53627, https://doi.org/10.7554/eLife.53627.

[22] G.M. Tannahill, A.M. Curtis, J. Adamik, E.M. Palsson-McDermott, A.F. McGettrick, G. Goel, C. Frezza, N.J. Bernard, B. Kelly, N.H. Foley, L. Zheng, A. Gardet, Z. Tong, S.S. Jany, S.C. Corr, M. Haneklaus, B.E. Caffrey, K. Pierce, S. Walmsley, F.C. Beasley, E. Cummins, V. Nizet, M. Whyte, C.T. Taylor, H. Lin, S.L. Masters, E. Gottlieb, V.P. Kelly, C. Clish, P.E. Auron, R.J. Xavier, L.A. O'Neill, Succinate is an inflammatory signal that induces IL-1β through HIF-1α, Nature 496 (7444) (2013 Apr 11) 238–242, https://doi.org/10.1038/nature11986.

[23] R. Zhou, A. Tardivel, B. Thorens, I. Choi, J. Tschopp, Thioredoxin-interacting protein links oxidative stress to inflammasome activation, Nat. Immunol. 11 (2) (2010 Feb) 136–140, https://doi.org/10.1038/ni.1831.

[24] L. Chantranupong, S.M. Scaria, R.A. Saxton, M.P. Gygi, K. Shen, G.A. Wyant, T. Wang, J.W. Harper, S.P. Gygi, D.M. Sabatini, The CASTOR proteins are arginine sensors for the mTORC1 pathway, Cell 165 (1) (2016 Mar 24) 153–164, https://doi.org/10.1016/j.cell.2016.02.035.